

Accurate Single Point Incremental Forming Simulations using Solid-Shell Elements

Carlos Felipe Guzmán¹, José Ilídio Velosa de Sena²,
Laurent Duchêne¹ and Anne Marie Habraken^{1,3}

¹Department ArGEnCo, division MS²F, Université de Liège, Belgium.

²Department of Mechanical Engineering, centre GRIDS, University of Aveiro, Portugal

³Research Director of the Fonds de la Recherche Scientifique-FNRS

September 11th, 2013



Presentation contents

1 Introduction

2 Simulations

3 Results

4 Conclusions

Contents

1 Introduction

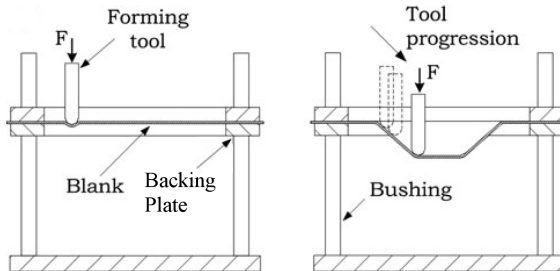
2 Simulations

3 Results

4 Conclusions

Single point incremental forming

- A sheet metal is deformed by a small tool.
- The tool could be guided by a CNC (milling machine, robot).



[Henrard et al., 2010]

Single point incremental forming

- **Dieless**, with high sheet formability.
- Easy shape generation.
- For rapid prototypes, small batch productions, etc.

Single point incremental forming

- **Dieless**, with high sheet formability.
- Easy shape generation.
- For rapid prototypes, small batch productions, etc.

Challenges

- Geometrical inaccuracy.
- Process mechanics.
- Increased formability.

Single point incremental forming

- **Dieless**, with high sheet formability.
- Easy shape generation.
- For rapid prototypes, small batch productions, etc.

Challenges

- Geometrical inaccuracy.
- Process mechanics.
- Increased formability.

Motivations

- Through the thickness gradient are important.
- 2D constitutive laws cannot be used.
- New advances on element formulation in FE codes.

Contents

1 Introduction

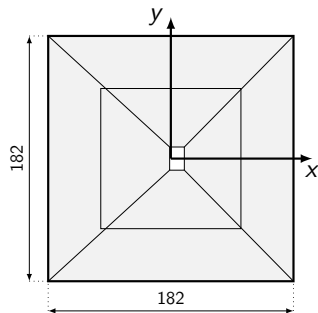
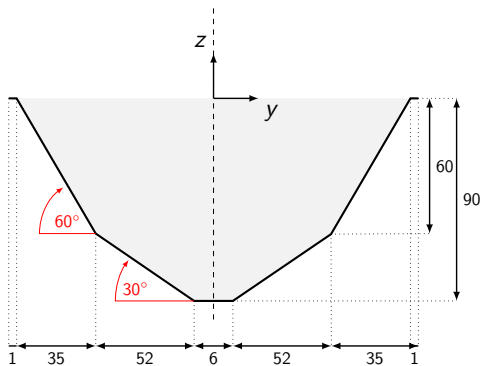
2 Simulations

3 Results

4 Conclusions

Simulations

- Material: DC01 ferritic steel (1 mm thickness).
- Two slope pyramid:



Constitutive modeling

- Isotropic elasto-plastic constitutive law (HILL3D_KI.F).
- Voce and Armstrong-Frederick isotropic/kinematic hardening.

$$\sigma_Y = \sigma_{Y0} + K (1 - \exp(-n\epsilon^P))$$

$$\dot{\mathbf{X}} = C_x \left(X_{sat} \dot{\epsilon}^P - \dot{\epsilon}^P \mathbf{X} \right)$$

Constitutive modeling

- Isotropic elasto-plastic constitutive law (HILL3D_KI.F).
- Voce and Armstrong-Frederick isotropic/kinematic hardening.

$$\sigma_Y = \sigma_{Y0} + K (1 - \exp(-n\epsilon^P))$$

$$\dot{\mathbf{X}} = C_x \left(X_{sat} \dot{\epsilon}^P - \dot{\epsilon}^P \mathbf{X} \right)$$

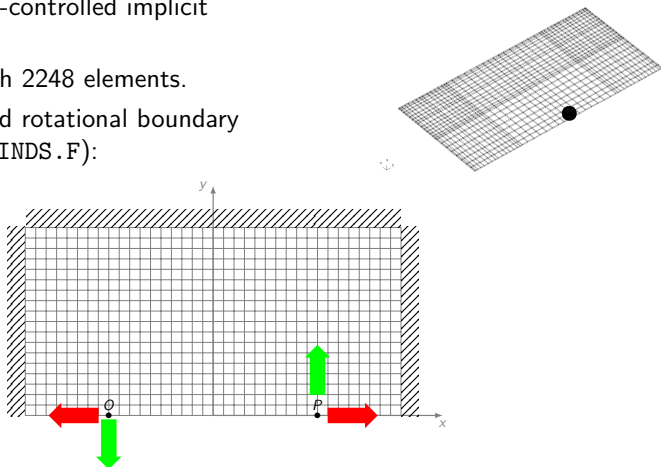
- Material parameters:

$$\begin{array}{llll} \sigma_{Y0} & = & 158 \text{ MPa} & C_x & = & 257 \\ K & = & 255 \text{ MPa} & X_{sat} & = & 4 \text{ MPa} \\ n & = & 13 & & & \end{array}$$

- Identification through *classical* (tensile, monotonic/Bauschinger shear) tests (OPTIM).

Mesh and boundary conditions

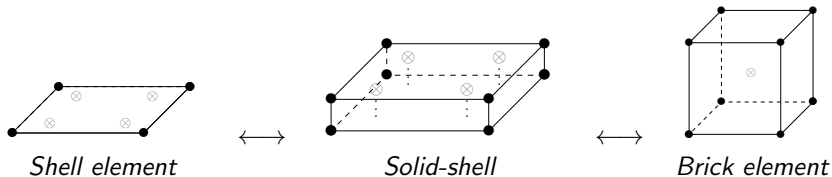
- Displacement-controlled implicit simulation.
- One layer with 2248 elements.
- Symmetry and rotational boundary conditions (BINDS.F):



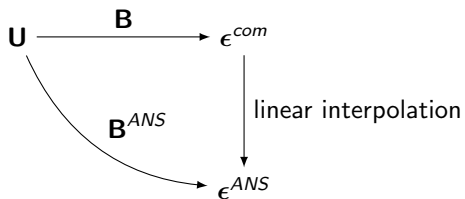
Solid-shell element

Formulation

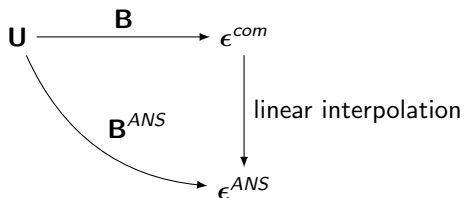
- Large aspect ratios \implies locking
- Enhanced Assumed Strain (EAS)
- Assumed Natural Strain (ANS)



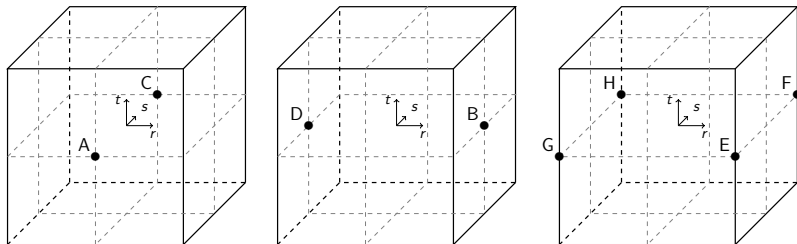
Assumed natural strain



Assumed natural strain



Sampling points (transverse shear and transverse normal strains):



Enhanced assumed strain

Enhanced strain field

$$\epsilon = \epsilon^{com} + \epsilon^{EAS}$$

$$\epsilon^{com} = \Delta^s \mathbf{u} = \mathbf{B}(r, s, t) \mathbf{U}$$

$$\epsilon^{EAS} = \mathbf{G}(r, s, t) \boldsymbol{\alpha} = \frac{|J_0|}{|J(r, s, t)|} \mathbf{F}_0^{-T} \mathbf{M}(r, s, t) \boldsymbol{\alpha}$$

Enhanced assumed strain

Enhanced strain field

$$\epsilon = \epsilon^{com} + \epsilon^{EAS}$$

$$\epsilon^{com} = \Delta^s \mathbf{u} = \mathbf{B}(r, s, t) \mathbf{U}$$

$$\epsilon^{EAS} = \mathbf{G}(r, s, t) \boldsymbol{\alpha} = \frac{|J_0|}{|J(r, s, t)|} \mathbf{F}_0^{-T} \mathbf{M}(r, s, t) \boldsymbol{\alpha}$$

$$\begin{array}{|c|c|c|c|c|c|c|c|c|c|c|c|c|c|c|c|c|c|c|c|c|c|c|c|c|} \hline
 r & 0 \\ \hline
 0 & s & 0 \\ \hline
 0 & 0 & t & 0 \\ \hline
 0 & 0 & 0 & r & s & 0 & 0 & 0 & 0 & 0 & rt & st & 0 & 0 & 0 & 0 & 0 & 0 & 0 & 0 & 0 & 0 & 0 & 0 \\ \hline
 0 & 0 & 0 & 0 & 0 & r & t & 0 & 0 & 0 & 0 & 0 & 0 & 0 & 0 & 0 & 0 & 0 & 0 & 0 & 0 & 0 & 0 & 0 \\ \hline
 0 & 0 & 0 & 0 & 0 & 0 & 0 & s & t & 0 & 0 & 0 & 0 & 0 & 0 & 0 & 0 & 0 & 0 & 0 & 0 & 0 & 0 & 0 \\ \hline
 \end{array}
 \quad
 \begin{array}{l}
 [\mathbf{M}] = \\
 \left[\begin{array}{cccccccccccccccccccccccccccc}
 rs & rt & 0 & 0 & 0 & 0 & 0 & 0 & 0 & 0 & 0 & 0 & 0 & 0 & 0 & 0 & 0 & 0 & 0 & 0 & rst & 0 & 0 & 0 & 0 & 0 \\
 0 & rst & 0 & 0 & 0 & 0 \\
 0 & rst & 0 & 0 & 0 \\
 0 & 0 & 0 & r & s & 0 & 0 & 0 & 0 & 0 & rt & st & 0 & 0 & 0 & 0 & 0 & 0 & 0 & 0 & 0 & 0 & 0 & 0 & rst & 0 & 0 \\
 0 & 0 & 0 & 0 & 0 & r & t & 0 & 0 & 0 & 0 & 0 & 0 & 0 & 0 & 0 & 0 & 0 & 0 & 0 & 0 & 0 & 0 & 0 & 0 & rst & 0 \\
 0 & 0 & 0 & 0 & 0 & 0 & 0 & s & t & 0 & 0 & 0 & 0 & 0 & 0 & 0 & 0 & 0 & 0 & 0 & 0 & 0 & 0 & 0 & 0 & 0 & rst
 \end{array} \right]
 \end{array}$$

03 EAS modes

Enhanced assumed strain

Enhanced strain field

$$\epsilon = \epsilon^{com} + \epsilon^{EAS}$$

$$\epsilon^{com} = \Delta^s \mathbf{u} = \mathbf{B}(r, s, t) \mathbf{U}$$

$$\epsilon^{EAS} = \mathbf{G}(r, s, t) \boldsymbol{\alpha} = \frac{|J_0|}{|J(r, s, t)|} \mathbf{F}_0^{-T} \mathbf{M}(r, s, t) \boldsymbol{\alpha}$$

$$\begin{bmatrix}
 r & 0 \\
 0 & s & 0 \\
 0 & 0 & t & 0 & 0 & 0 & 0 & 0 & 0 & 0 & 0 & 0 & 0 & 0 & 0 & 0 & 0 & 0 & 0 & 0 & 0 & 0 \\
 0 & 0 & 0 & r & s & 0 & 0 & 0 & 0 & rt & st & 0 & 0 & 0 & 0 & 0 & 0 & 0 & 0 & 0 & 0 & 0 \\
 0 & 0 & 0 & 0 & 0 & r & t & 0 & 0 & 0 & 0 & 0 & 0 & 0 & 0 & 0 & 0 & 0 & 0 & 0 & 0 & 0 \\
 0 & 0 & 0 & 0 & 0 & 0 & 0 & s & t & 0 & 0 & 0 & 0 & 0 & 0 & 0 & 0 & 0 & 0 & 0 & 0 & 0
 \end{bmatrix}$$

11 EAS modes

Enhanced assumed strain

Enhanced strain field

$$\boldsymbol{\epsilon} = \boldsymbol{\epsilon}^{com} + \boldsymbol{\epsilon}^{EAS}$$

$$\boldsymbol{\epsilon}^{com} = \Delta^s \mathbf{u} = \mathbf{B}(r, s, t) \mathbf{U}$$

$$\boldsymbol{\epsilon}^{EAS} = \mathbf{G}(r, s, t) \boldsymbol{\alpha} = \frac{|J_0|}{|J(r, s, t)|} \mathbf{F}_0^{-T} \mathbf{M}(r, s, t) \boldsymbol{\alpha}$$

$$[\mathbf{M}] =$$

$$\begin{bmatrix} r & 0 & 0 & 0 & 0 & 0 & 0 & 0 & 0 & 0 & 0 & 0 & 0 & 0 & 0 & rs & rt & 0 & 0 & 0 & 0 & 0 & 0 & 0 & 0 & rst & 0 & 0 & 0 & 0 & 0 & 0 \\ 0 & s & 0 & rst & 0 & 0 & 0 & 0 \\ 0 & 0 & t & 0 \\ 0 & 0 & 0 & r & s & 0 & 0 & 0 & 0 & rt & st & 0 & 0 & 0 & 0 & 0 & 0 & 0 & 0 & 0 & 0 & 0 & 0 & 0 & rs & 0 & 0 & 0 & 0 & 0 & 0 & 0 \\ 0 & 0 & 0 & 0 & 0 & r & t & 0 & 0 & 0 & 0 & 0 & rs & st & 0 & 0 & 0 & 0 & 0 & 0 & 0 & 0 & 0 & 0 & 0 & 0 & 0 & 0 & 0 & 0 & 0 & 0 \\ 0 & 0 & 0 & 0 & 0 & 0 & 0 & s & t & 0 & 0 & 0 & 0 & 0 & 0 & rs & rt & 0 & 0 & 0 & 0 & 0 & 0 & 0 & 0 & 0 & 0 & 0 & 0 & 0 & 0 & 0 \end{bmatrix}$$

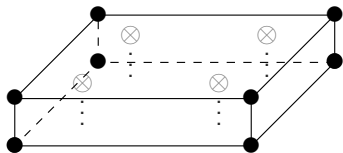
24 EAS modes

Solid-shell element

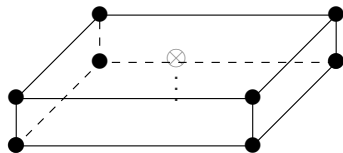
... in LAGAMINE

Enhanced Assumed Strain (EAS) modes
Assumed Natural Strain (ANS) version
In-plane integration
Stabilization technique

SSH3D	RESS
24	1
4	-
full	reduced*
-	Yes



SSH3D.F



RESS3.F

Running simulations

Not easy...

- Complex toolpath and small contact zone.
- Several time increments.
- Simulations can take **weeks**.

Running simulations

Not easy...

- Complex toolpath and small contact zone.
- Several time increments.
- Simulations can take **weeks**.

NIC machine

- Near 1000 cores and 5 Tb memory.
- LAGAMINE (and PREPRO) compiled in Linux.
- Possibility of using other machines (Lemaître-UCL,...)



Contents

1 Introduction

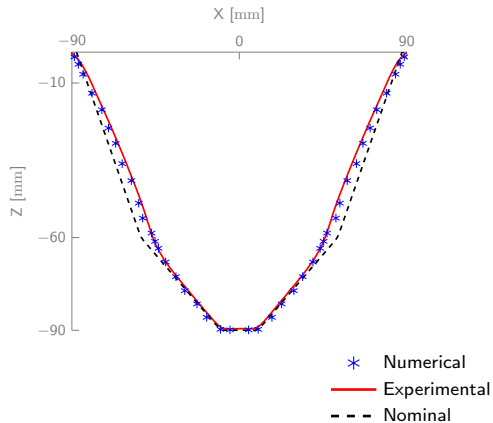
2 Simulations

3 Results

4 Conclusions

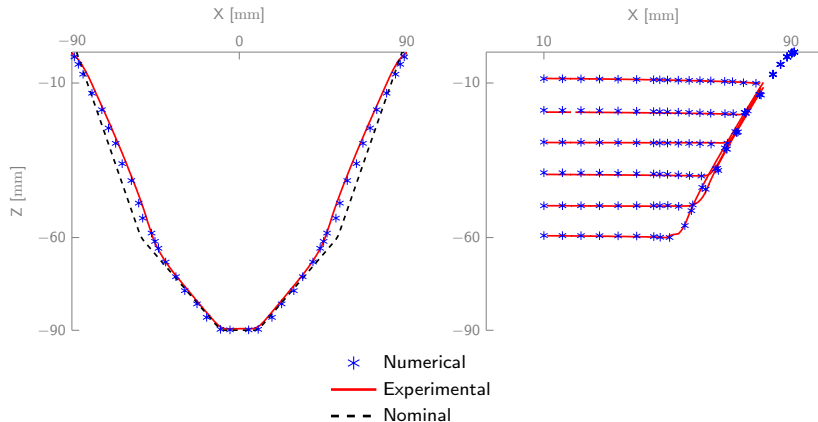
Shape results

Numerical/experimental (DIC) comparison $Y = 0$



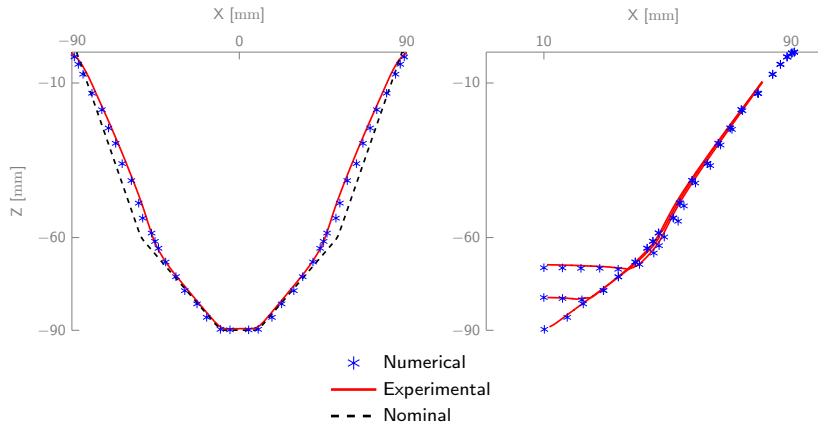
Shape results

Numerical/experimental (DIC) comparison $Y = 0$



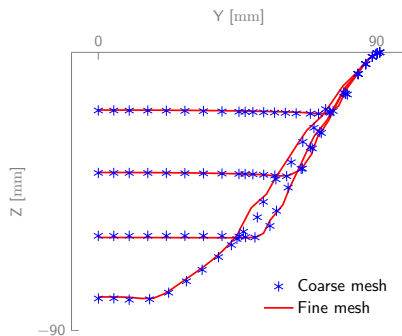
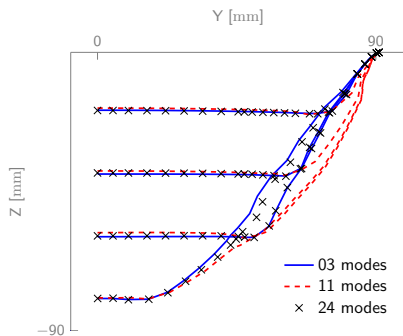
Shape results

Numerical/experimental (DIC) comparison $Y = 0$



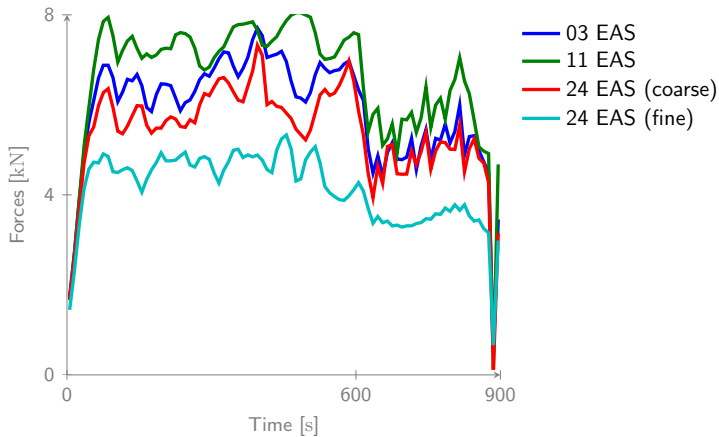
EAS and mesh influence

- Strong EAS mode influence.
- Small mesh influence.



Force evolution

- Both EAS modes and mesh influence.



Contents

1 Introduction

2 Simulations

3 Results

4 Conclusions

Conclusions

- EAS modes influence the accuracy of the results.
- The elements are subjected to deformation modes reproduced only using the EAS technique.
- ANS version has no effect on both the shape and the force.
- Material identification procedure important.

Conclusions

- EAS modes influence the accuracy of the results.
- The elements are subjected to deformation modes reproduced only using the EAS technique.
- ANS version has no effect on both the shape and the force.
- Material identification procedure important.

Future work

- Identify the most important EAS modes.
- Improve identification procedure to consider out-of-plane stresses.

Accurate Single Point Incremental Forming Simulations using Solid-Shell Elements

Carlos Felipe Guzmán¹, José Ilídio Velosa de Sena²,
Laurent Duchêne¹ and Anne Marie Habraken^{1,3}

¹Department ArGEnCo, division MS²F, Université de Liège, Belgium.

²Department of Mechanical Engineering, centre GRIDS, University of Aveiro, Portugal

³Research Director of the Fonds de la Recherche Scientifique-FNRS

September 11th, 2013



References

Henrard, C., Bouffioux, C., Eyckens, P., Sol, H., Duflou, J., van Houtte, P., Van Bael, A., Duchêne, L., Habraken, A. M., Dec. 2010. Forming forces in single point incremental forming: prediction by finite element simulations, validation and sensitivity. *Computational Mechanics* 47 (5), 573–590.